Journal of
Emerging Investigators

Fabrication of $CuSbS_2$ Solar Cells by Sulfurization of Thermally Evaporated Metal Stacks

Mariam Abou-Dahech[1], Nicholas Franzer[2], Rajendra Khanal[2], Adam Phillips[2], and Yanfa Yan[2]

[1]Toledo Early College High School, Toledo, OH

[2]University of Toledo, Toledo, OH

Summary

We report on the deposition of thin films of chalcostibite ($CuSbS_2$) created by sulfurization of thermally evaporated metal stacks. We found by X-ray diffraction that thermally evaporated copper and antimony metal films, which were annealed for 1.5 hours at 400°C followed by rapid sulfurization at 400°C for 15 minutes, exhibit the $CuSbS_2$ crystalline phase. The films have high optical absorption with a band gap of ~1.6 eV. Our $CuSbS_2$-based thin film solar cells had low conversion efficiency, due to the formation of a layer of molybdenum disulfide (MoS_2) and/or secondary phases at the molybdenum back contact layer–$CuSbS_2$ interface. To negate this problem, we applied a layer of single-walled carbon nanotubes (SWCNT) on the molybdenum back contact. This arrangement allowed for a better junction between the molybdenum and $CuSbS_2$ layers. With the addition of SWCNT, our best cell under AM 1.5 illumination exhibited an open circuit voltage (V_{oc}) of 321 mV, a short circuit current density (J_{sc}) of 3.76 mA/cm^2, and a fill factor of 27%, resulting in a conversion efficiency of 0.33%. This work shows that for effective solar devices, it is critical that device layers are electrically aligned to allow for better electron passage. In the case presented here, we increased the efficiency by creating a passageway for electrons through the device by eliminating the formation of MoS_2. This can be achieved by inserting single-walled carbon nanotubes (SWCNTs) that allow a better junction between the molybdenum and $CuSbS_2$ layers. An alternative may include changing sulfur quantity, sulfurization time, or temperature.

Received: September 21, 2015; **Accepted:** March 24, 2016; **Published:** July 19, 2016

Copyright: (C) 2016 Abou-Dahech, Franzer, Khanal, Phillips, and Yan. All JEI articles are distributed under the attribution non-commercial, no derivative license (http://creativecommons.org/licenses/by-nc-nd/3.0/). This means that anyone is free to share, copy and distribute an unaltered article for non-commercial purposes provided the original author and source is credited.

Introduction

Photovoltaics produce power by converting the sun's energy into electrical power. Visible light is absorbed by material with a lower band gap than the light's energy. The light travels through the other layers in the device with higher band gaps until it reaches the lower band gap layer. Once light with energy greater than the band gap of the semiconductor is absorbed, an electron-hole pair is created (**Figure 1a**). An electric field produced at the junction of the N-type and P-type layers drives the electron and hole to opposite ends of the device where the conductors are located. The electron-hole pair then can be extracted to power a load (1). A high resistivity transparent layer is included to prevent direct contact of the two conductors present in the devices in case of holes in any layers.

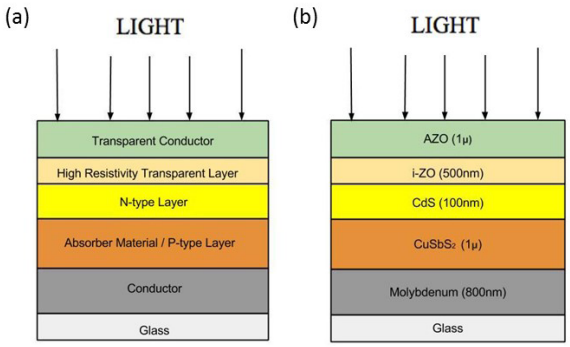

Figure 1. (a) Illustration of the parts of a photovoltaic device. **(b)** A depiction of the individual layers that a $CuSbS_2$ device is comprised of.

Currently, silicon and thin film, such as cadmium telluride (CdTe), panels dominate the photovoltaic market. Silicon solar panels are made from wafers that must be highly purified, causing their production to be expensive (2), and thin films use rare or expensive elements (3). Therefore, investigating emerging photovoltaic technologies using nontoxic and economically viable elements is warranted.

In this study, we used chalcostibite ($CuSbS_2$) as an absorbing material in a photovoltaic (PV) device because of its feasibility and relatively abundant nature (4). With a band gap similar to that of CdTe, $CuSbS_2$ is expected to absorb a similarly large portion of the solar spectrum. Additionally, it is less expensive due to more earth-abundant source materials. The $CuSbS_2$ was fabricated by thermally evaporating copper and antimony, followed by annealing and sulfurization; this technique generated large grain $CuSbS_2$. For device fabrication, $CuSbS_2$ was deposited on molybdenum-coated soda lime glass in substrate configuration (**Figure 1b**). The $CuSbS_2$ device

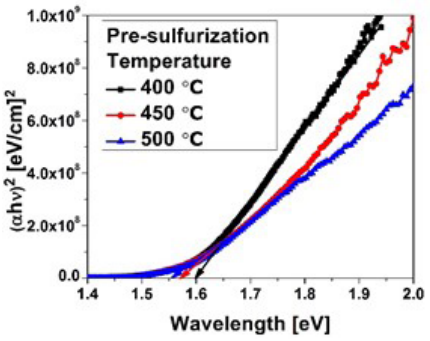

Figure 2. Graphical representation of the $(\alpha h\upsilon)^2$ vs hu for the three temperatures. By extrapolating the data to the x-intercept, it is clear that the band gap is ~1.6 eV for all annealing temperatures. This is near the ideal band gap for solar conversion.

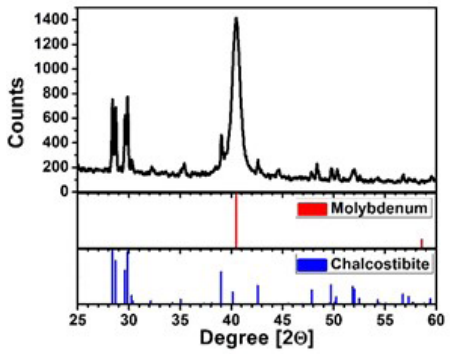

Figure 3. X-ray diffraction spectrum of metal stacks annealed and rapidly sulfurized. Each peak characterizes a crystal plane within the material's overall crystal lattice in the film.

was completed with 100 nm of cadmium sulfide (CdS), 500 nm of intrinsic zinc oxide (i-ZnO), and 1 micron of aluminum zinc oxide (AZO). The completed devices exhibited low efficiency due to the formation of a layer consisting MoS_2 and secondary phases (compounds that consist of Cu, Sb, and/or S that are not $CuSbS_2$, e.g. CuS_2 or CuS) at the back contact during sulfurization similar to what others have observed with a related materials system (5). Inserting single-walled carbon nanotubes (SWCNTs) between the Mo and $CuSbS_2$ layers limited the MoS_2 formation (6) and resulted in increased efficiency.

Results and Discussion

Film Characterization

After the fabrication of our devices, several tests were needed in order to characterize the finished solar cells. We first determined the optical and crystal structure properties of our materials.

The absorption coefficient was determined, and the results were used to generate **Figure 2**, which shows the square of the photon energy multiplied by the optical absorption across wavelengths. Because $CuSbS_2$ is a direct band gap semiconductor, the x-intercept of the linear portion is its band gap. This absorption spectrum ultimately illustrates a high optical absorption by the material produced by all three annealing temperatures. A straight line was added to see what band gap our extrapolation hits. We determined that the band gap of the $CuSbS_2$ layer is ~1.6 eV, which is a near ideal band gap for our absorbing material, $CuSbS_2$. Next, we utilized the X-ray diffraction (XRD) instrument in order to characterize the structure of the synthesized material. **Figure 3** shows the measured XRD data on the top and the reference signals of crystalline Mo and $CuSbS_2$ (the material we deposited on and the material we created, respectively) on the bottom. Since our peak locations of the measured data matched the standards, with roughly the same height and position, we confirmed that we had crystalline Mo (with a very strong peak at ~41°) and $CuSbS_2$ (with pairs of peaks at ~28° and 30°), which is the material we were trying to make.

Solar Cell Performance

Knowing that we created $CuSbS_2$ with a 1.6 eV band gap, we investigated how a device made with this material operated under direct sunlight. Complete devices were made using 400°C annealing conditions. The dark and illuminated current densities-voltage curves (J-V) were measured to determine the conversion efficiency of the solar cells (**Figure 4a**). Ideally, each photon above the band gap should result in the generation of one electron. By integrating all the photons in the solar spectrum at the surface of the earth (AM 1.5) with energy greater than the band gap of our material, 1.6 eV, we would expect 22 mA/cm^2 (7). Our device resulted in a J_{sc} (the y-intercept) of 0.758, which is extremely low. Many of the photons did not yield electrons in our device. If the solar cell is efficient the results would follow a classic diode curve, in which the current density (shown on the y-axis) would be nearly constant before sharply decreasing. The measured J-V response of this device, though, is linear. This could be due to high series resistance caused by a resistive layer preventing electron movement or by a

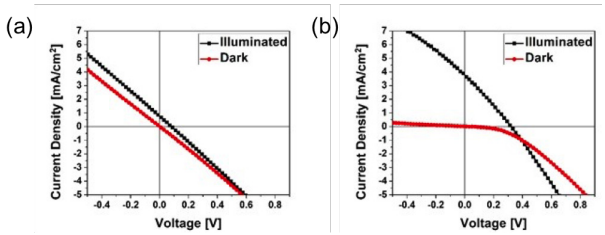

Figure 4. J-V curve of the best $CuSbS_2$-based thin-film solar cell **(a)** without SWCNTs and **(b)** with SWCNTs at the molybdenum and $CuSbS_2$ junction.

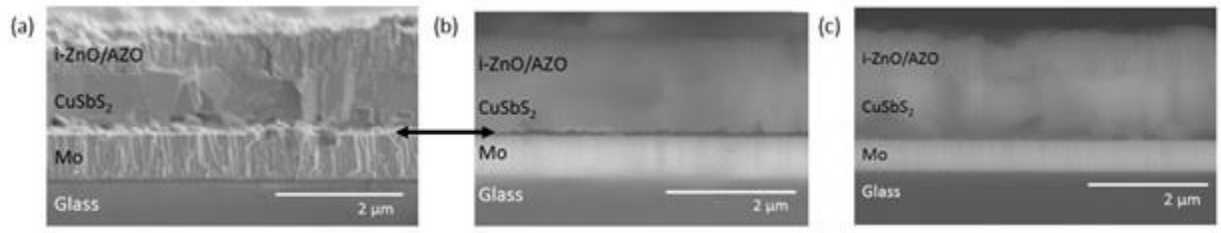

Figure 5. Cross-sectional SEM (a) and backscattering electron (b) images indicate an insulating layer (shown by black arrow) between the $CuSbS_2$ and molybdenum. This is likely MoS_2 formed during sulfurization. Backscattering electron image of the materials stack with single-wall carbon nanotubes (c) does not show the insulating layer.

very low shunt resistance caused by low quality material, which both result in a low fill factor.

In order to determine what the problem was with our device, we used cross-sectional scanning electron microscopy (SEM) (shown in **Figure 5a-b**). Each layer of the device (see **Figure 1b** for reference) is shown in this SEM image (**Figure 5a**), except the n-layer because it is thin and partially diffused into the absorber layer. In this image, the $CuSbS_2$ is the large layer in the center, and the smaller one towards the bottom is the molybdenum. For our device to work, the $CuCbS_2$ and Mo layers must be in good electrical contact. According to the backscattering image (**Figure 5b**), there is a small dark layer (which indicates a poor conductivity layer) between the $CuSbS_2$ and Mo layers, likely composed of MoS_2 and other Cu-, Sb-, Mo-, and S-containing secondary phases, which prevents contact between the conductor (Mo) and the P-type layer ($CuSbS_2$), similar to what others have observed (5). Without this connection, the electrons cannot successfully pass through opposite ends of the device to be extracted and to power a load. It should be noted that the XRD peak for MoS_2 (~12°) is below the measured range, so the MoS_2 was not verified.

To eliminate the problem of unsuccessful electron passage through the device, a layer of single-wall carbon nanotubes (SWCNTs) was deposited on the molybdenum prior to $CuSbS_2$ deposition. SWCNTs have recently been used to form good electrical contacts to other solar cell materials even though the simple band alignment predictions would suggest otherwise (8 - 9). Here, they could increase the efficiency by either forming good electrical contacts or by limiting the extent to which S interacts with Mo (6). In either case, these tubes serve as a passageway for electrons so that they can get to the $CuSbS_2$ layer of the device. Unlike the cross sectional backscattering image of the device without SWCNTs (**Figure 5b**), the cross sectional backscattering image of the device with SWCNTs (**Figure 5c**) does not show the dark line indicating an insulating layer between the $CuSbS_2$ and the Mo layer. We interpret this to mean that the SWCNTs prevented MoS_2 formation between the molybdenum and $CuSbS_2$.

With no MoS_2 layer or secondary phases evident, we expected the device with the SWCNT layer to perform better, providing that the SWCNT layer does not adversely affect charge transport. In the J-V curve of the device with SWCNTs, shown in **Figure 4b**, the current density line (y-axis) better mirrors the theoretical graph of an efficient solar cell; the graph is no longer linear. Comparing the results of these devices in **Table 1**, we see that the carbon nanotubes had a positive effect on the solar cells' efficiency. With this information, we conclude that our solar cells with SWCNTs are significantly more efficient than the solar cells without nanotubes. However, since our material has the capability of reaching a 22 mA/cm^2 current density, and based on the 3.764 mA/cm^2 density our device actually reached, we also believe that the efficiency of our device is lower than it could be.

Conclusion

$CuSbS_2$ thin film devices created by thermal evaporation have been characterized by their optical and structural properties. $CuSbS_2$ films demonstrate high optical absorption, with a band gap of ~1.6 eV and a 400°C anneal having stronger absorption. During the fabrication of our solar devices, a layer of MoS_2 formed at the molybdenum/$CuSbS_2$ junction, preventing a significant PV response. Application of SWCNTs on the molybdenum reduced the formation of MoS_2 and allowed for a better electrical junction between the molybdenum and $CuSbS_2$. This enabled us to get a solar cell efficiency of 0.33% under AM 1.5 illumination. Further optimization

Performance Parameters	Without SWCNTs	With SWCNTs
V_{oc} (V)	0.086	0.321
J_{sc} (mA/cm^2)	0.758	3.764
Fill Factor (%)	24.8	27.0
Efficiency (%)	0.016	0.326

Table 1. Performance parameters of the best $CuSbS_2$-based thin-film solar cell with and without SWCNT at the molybdenum and $CuSbS_2$ junction.

of the device is needed so that the layer of MoS_2 will not form and interfere with cell performance. Optimizing the molybdenum and $CuSbS_2$ junction by varying the thickness of the carbon nanotubes (9) or by finding an alternative layer that prevents formation of MoS_2 are two ways this can be achieved. Changing the amount of sulfur used or the sulfurization time and temperature may also result in better device performance.

Methods

Material Characterization

$CuSbS_2$ was fabricated on soda lime glass substrates. Prior to deposition, the soda lime glass was ultrasonically cleaned using an ammonium-based solution. Copper and antimony layers were thermally evaporated in a three-layer metal stack sequence. Previous experiments indicated that 75 nm of copper, 250 nm of antimony, and 25 nm of copper result in the best film. The stacks were then annealed to induce mixing of the metal stack. The samples were annealed in a argon purged furnace. The temperature ramp time was 1.5 hours, and the dwell time was 30 minutes. Three different temperatures, 400, 450, and 500°C, were tested to determine the optimum annealing conditions. The samples were allowed to cool before sulfurization. Sulfurization was completed in a graphite box containing 0.15 g of sulfur powder and heated to 400°C for 15 minutes in argon ambient using a rapid thermal annealer. This caused the films to crystallize into a 1-μm thick $CuSbS_2$ film. The films were characterized by X-ray Diffraction (XRD) and a UV-Vis Spectrophotometer. The XRD was set to focus beam mode with a sweep rate of 1°/min. The data was obtained in air at room temperature.

Optical absorption determination

When light enters the device, absorption takes place. By calculating this absorption, we confirmed our band gap. The band gap from our absorbing material, $CuSbS_2$, determines the minimum amount of energy a photon must have in order to be absorbed. The optical absorption (α) was used to determine the band gap of the material produced by each annealing temperature using equation 1 (10).

$$\alpha = \frac{1}{d}\ln\left(\frac{\sqrt{(1-R)^4 + 4T^2R^2} - (1-R)^2}{2TR^2}\right) \quad (1)$$

Where d is the film thickness, and R and T are the reflectance and transmission, respectively.

Solar Cell Fabrication

An 800-nm molybdenum back contact was sputtered on the SLG using Radio Frequency (R.F.) magnetron sputtering. The $CuSbS_2$ was then deposited following the process noted above. A 100-nm thick CdS window layer was deposited on the $CuSbS_2$ using a chemical bath deposition (CBD) technique (11), and the device was completed by R.F. sputtering of 500 nm i-ZnO and 1μm AZO. Dot cells with an area of 0.09 cm^2 were then prepared by mechanically scribing. The finished devices were characterized by imaging the cross-sections of devices that were cracked in half. The SEM samples were prepared by scribing the glass on the opposite side of the device materials and cracking with a glass cracking tool. The samples were mounted onto a vertical holder that pointed the sample edge towards the electron beam using copper tape to provide the required conductivity. To acquire the SEM image of the surface, the accelerating potential and working distance were set to 2 kV and 11 mm, respectively. For the backscattering measurements, the accelerating potential was increased to 20 kV and the working distance was set to 25 mm. The J-V response was measured under a solar simulator with an AM 1.5 illumination, which is equivalent to that at the surface of the earth.

Acknowledgements

This work was supported by the Research In Science & Engineering (RISE) program at the University of Toledo, with financial assistance from UT's College of Natural Science and Mathematics, the National Science Foundation (No. 1230246), and discretionary funds from Profs. Ellingson, Heben, and Yan.

References

1. Luque, Antonio. *Handbook of Photovoltaic Science and Engineering*. Chichester: Wiley, 2003. Print.
2. Saga, Tatsuo. "Advances in Crystalline Silicon Solar Cell Technology for Industrial Mass Production." *NPG Asia Materials* 2.3 (2010): 96-102. Print.
3. "National Center for Photovoltaics." NREL. N.p., 5 June 2015. Web. 01 Aug. 2015.
4. Yang, Bo, Liang Wang, Jun Han, Ying Zhou, Huaibing Song, Shiyou Chen, Jie Zhong, Lu Lv, Dongmei Niu, and Jiang Tang. "CuSbS2 as a Promising Earth-Abundant Photovoltaic Absorber Material: A Combined Theoretical and Experimental Study." *Chemistry of Materials* (2014): 3135-143. Print.
5. Scragg, Jonathan J., J. Timo Wätjen, Marika Edoff, Tove Ericson, Tomas Kubart, and Charlotte Platzer-Björkman. "A Detrimental Reaction at the Molybdenum Back Contact in Cu2ZnSn(S,Se) 4 Thin-Film Solar Cells." *Journal of the American Chemical Society* 134.47 (2012): 19330-9333. Print.
6. X. L. Liu, H. T. Cui, W. Li, N. Song, F. Y. Liu, G. Conibeer and X. J. Hao *Physica Status Solidi-Rapid*

Research Letters 8, (2014).
7. "Spectrum Library." *PV Lighthouse*. N.p., n.d. Web. 17 Sept. 2015.
8. Phillips, Adam B., Rajendra R. Khanal, Zhaoning Song, Rosa M. Zartman, Jonathan L. Dewitt, Jon M. Stone, Paul J. Roland, Victor V. Plotnikov, Chad W. Carter, John M. Stayancho, Randall J. Ellingson, Alvin D. Compaan, and Michael J. Heben. "Wiring-up Carbon Single Wall Nanotubes to Polycrystalline Inorganic Semiconductor Thin Films: Low-Barrier, Copper-Free Back Contact to CdTe Solar Cells." *Nano Letters* 13.11 (2013): 5224-232. Print.
9. Schulz, Philip, Anne-Marie Dowgiallo, Mengjin Yang, Kai Zhu, Jeffrey L. Blackburn, and Joseph J. Berry. "Charge Transfer Dynamics between Carbon Nanotubes and Hybrid Organic Metal Halide Perovskite Films." *The Journal of Physical Chemistry Letters* 7.3 (2016): 418-25. Print.
10. Kharroubi, B., R. Baghdad, A. Abdiche, M. Bousmaha, M. Bousquet, A. Zeinert, M. El Marssi, K. Zellama, and S. Hamzaoui, "Mn Doping Effect on the Structural Properties of ZnO-nanostructured Films Deposited by the Ultrasonic Spray Pyrolysis Method." *Physica Scripta* 86.1 (2012): 015805. Web.
11. Chu, T. L. "Solution-Grown Cadmium Sulfide Films for Photovoltaic Devices." *Journal of The Electrochemical Society* 139.9 (1992): 2443-446. Print.